Figure S1

A

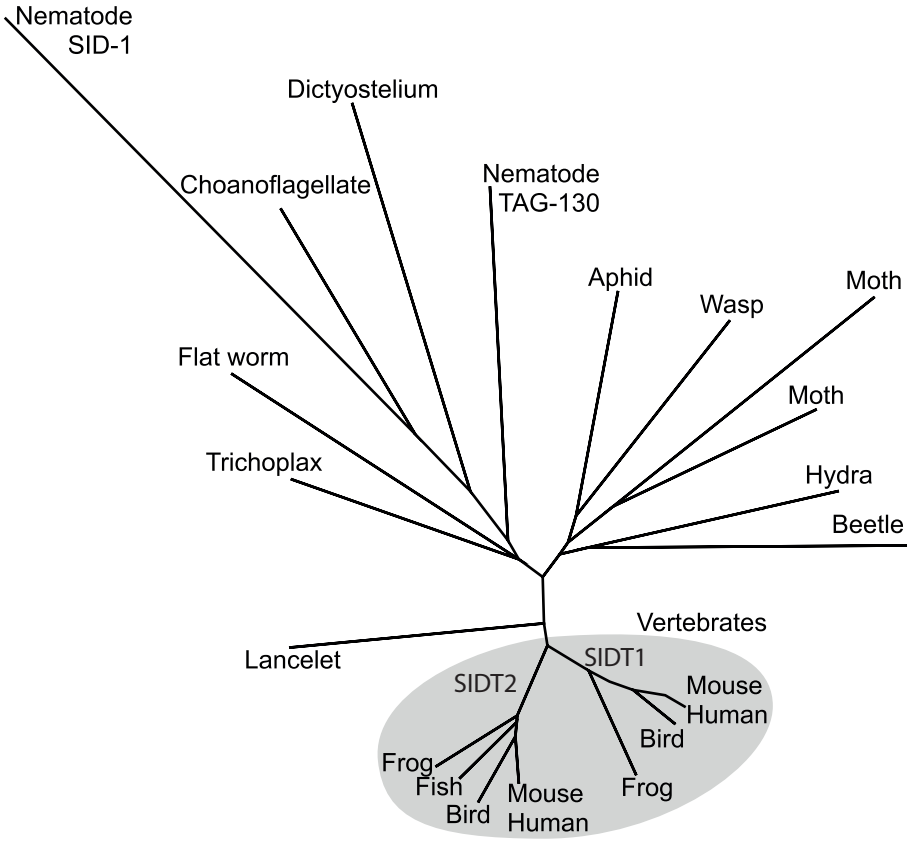
Nematode
SID-1
Dictyostelium
Choanoflagellate
Nematode
TAG-130
Aphid
Wasp
Moth
Flat worm
Moth
Trichoplax
Hydra
Beetle
Vertebrates
Lancelet
SIDT1
SIDT2
Mouse
Human
Bird
Frog
Fish
Bird
Mouse
Human
Frog

B

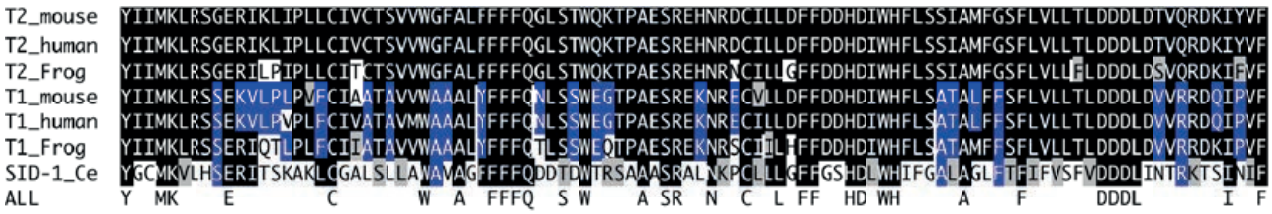
T2_mouse
T2_human
T2_Frog
T1_mouse
T1_human
T1_Frog
SID-1_Ce
ALL

Figure S1 – *C. elegans* SID-1 is conserved across diverse animal species, and its vertebrate orthologs, SIDT1 and SIDT2, are closely related.
(Related to "SID-1 family members: phylogenetic analysis" in STAR Methods)
(A) Radial-tree display of aligned SID-1 homologous gene sequences by neighbour joining. SID-1 homologs are detected in nearly all sequenced animal phyla (including the primitive metazoan, Trichoplax, as well as choanoflagellates and Dictyostelium) but remain undetected in Diptera, Ascidiacea, plants, and prokaryotes**. (B)** Sequence identity (black background), similarity (grey) and SIDT1-specific differences (blue) of carboxy-terminal 100 amino acids (T1=SIDT1, T2=SIDT2, Ce=*C. elegans*). Identical amino acids in all seven sequences are shown at the bottom.

Figure S2

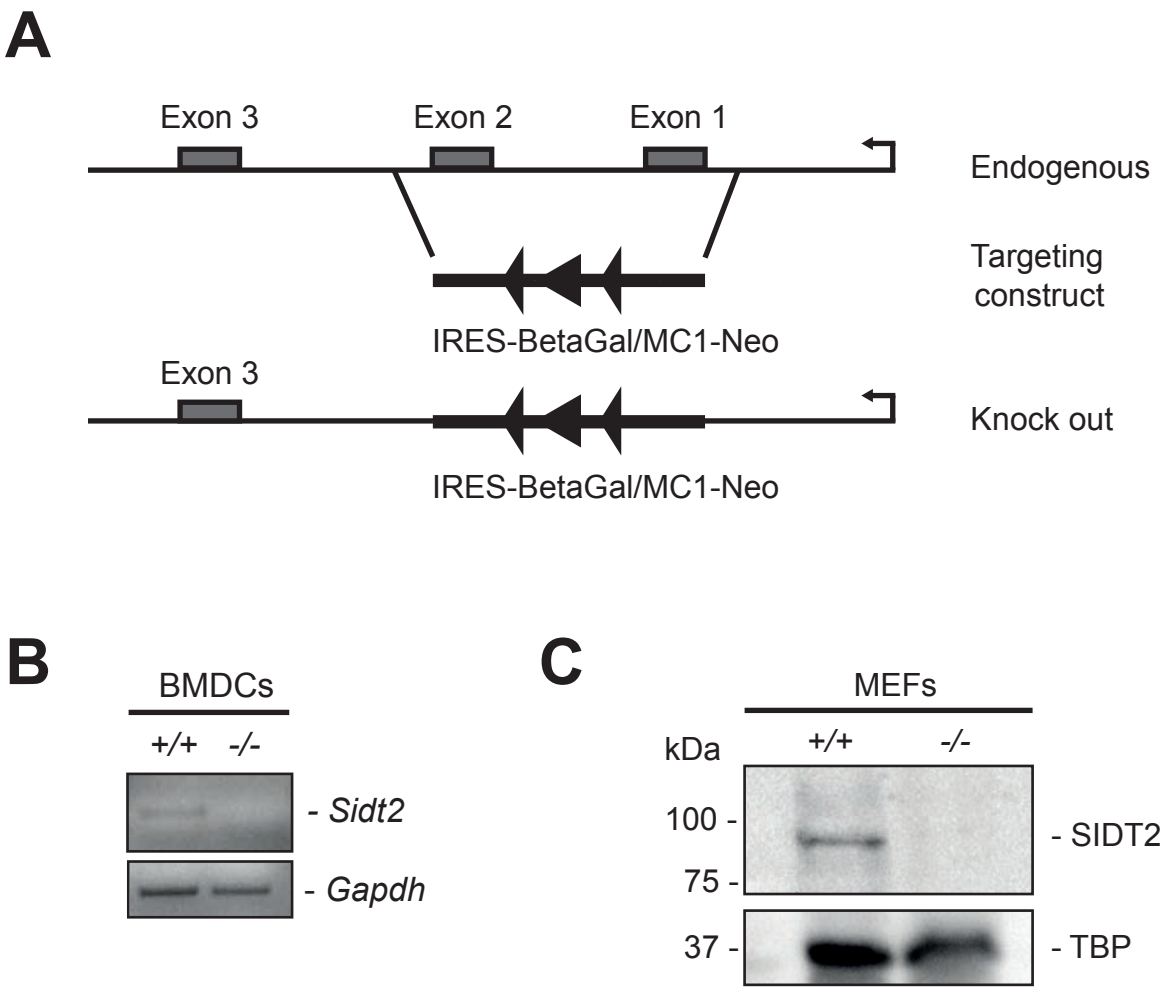
A
Exon 3
Exon 2
Exon 1
Endogenous
Targeting construct
IRES-BetaGal/MC1-Neo
Exon 3
Knock out
IRES-BetaGal/MC1-Neo
B
BMDCs
+/+
-/-
- Sidt2
- Gapdh
C
MEFs
kDa
+/+
-/-
100 -
75 -
- SIDT2
37 -
- TBP

Figure S2 – Targeting strategy and validation of *Sidt2*$^{-/-}$ mice.
(Related to Figures 2,3,4, 6 and 7)
(A) Schematic of the endogenous *Sidt2* allele, *Sidt2* targeting construct, and mutated *Sidt2* allele following replacement of exons 1 and 2 with a LacZ-neomycin cassette. **(B)** RT-PCR analysis of *Sidt2* mRNA in *Sidt2*$^{+/+}$ and *Sidt2*$^{-/-}$ BMDCs following 30 amplification cycles. *Gapdh* mRNA served as a positive control. **(C)** Western blot analysis of SIDT2 protein in *Sidt2*$^{+/+}$ and *Sidt2*$^{-/-}$ MEFs following digitonin treatment and subsequent immunoprecipitation (IP) of SIDT2. TBP protein from the lysis buffer prior to IP served as an input control. Expected size of SIDT2: 95 kDa.

Figure S3

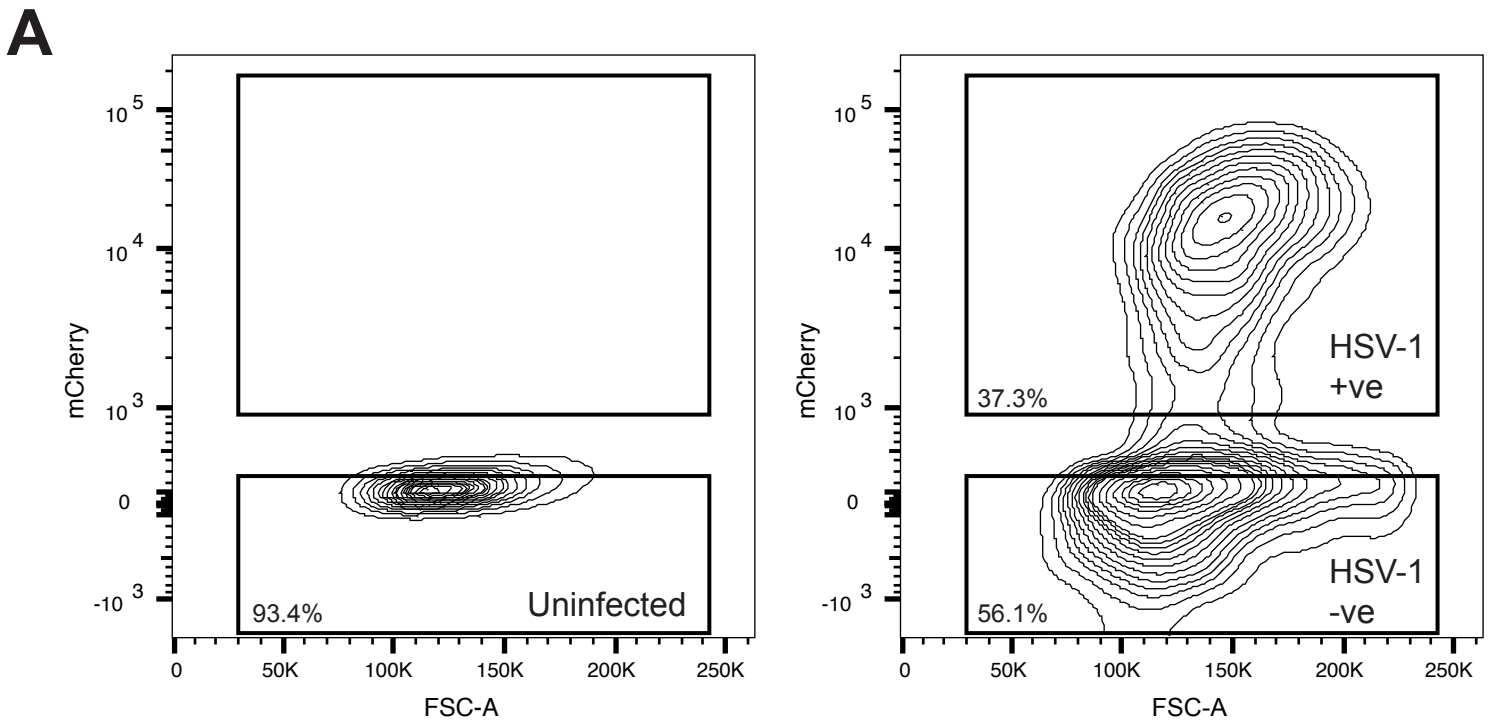
A
mCherry
FSC-A
93.4%
Uninfected
37.3%
HSV-1
+ve
56.1%
HSV-1
-ve

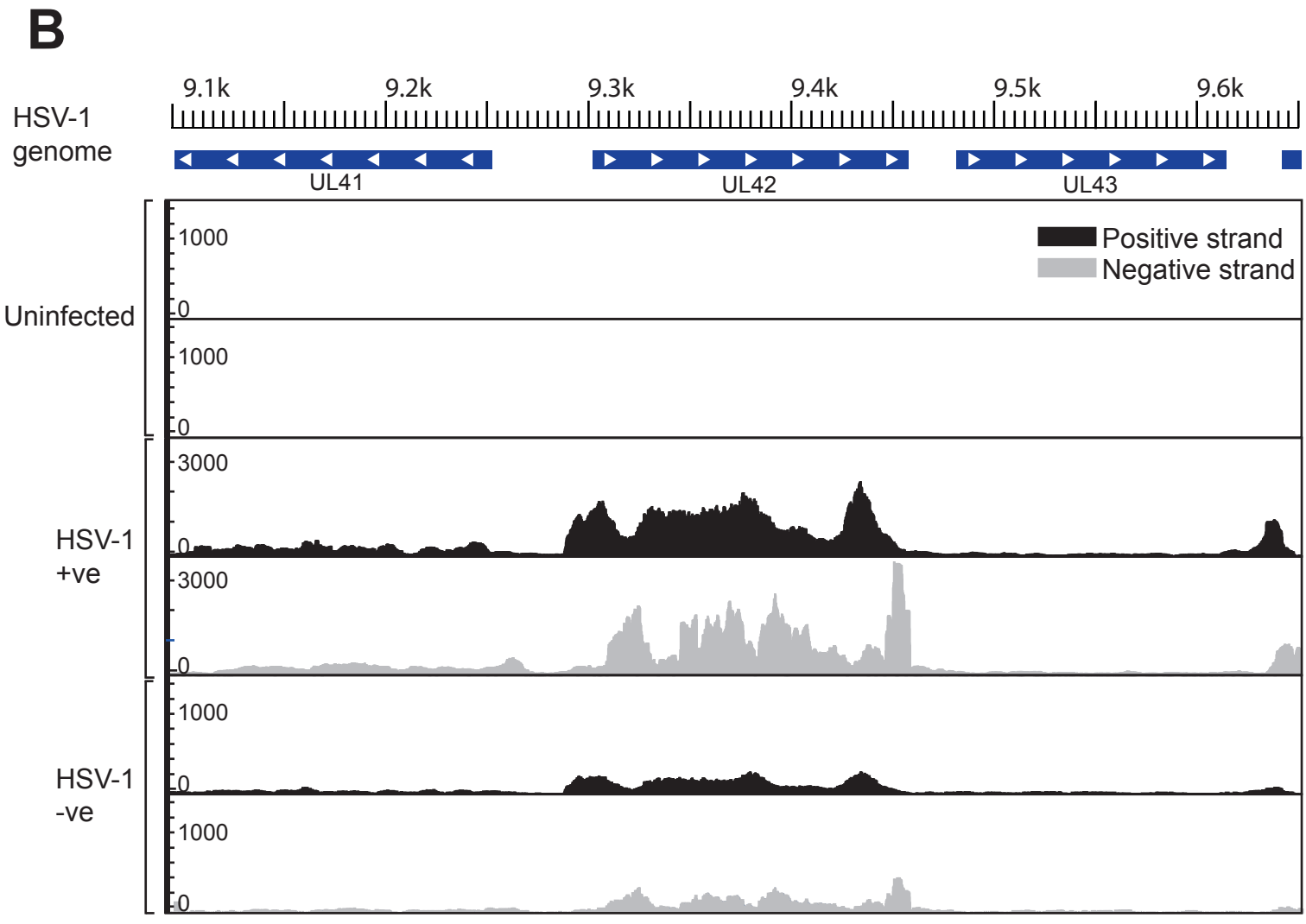
B
HSV-1
genome
9.1k
9.2k
9.3k
9.4k
9.5k
9.6k
UL41
UL42
UL43
Positive strand
Negative strand
Uninfected
HSV-1
+ve
HSV-1
-ve

Figure S3 – HSV-1 viral dsRNA is detectable in HSV-1$^-$ bystander cells.
(Related to Figure 2)

(A) Vero cells were infected with 0.5 MOI HSV-1-GFP for 48 h (right panel) and HSV-1$^+$ and HSV-1$^-$ cells isolated by fluorescence-activated cell sorting (FACS). As a negative control, uninfected Vero cells were also isolated (left panel). **(B)** Representative RNAseq coverage plots from HSV-1$^+$, HSV-1$^-$ and uninfected Vero cells of the HSV-1 genome are shown. To determine the presence of double-stranded RNAs, stranded RNAseq was performed in order to distinguish between reads from the positive strand and the negative strand.

Figure S4

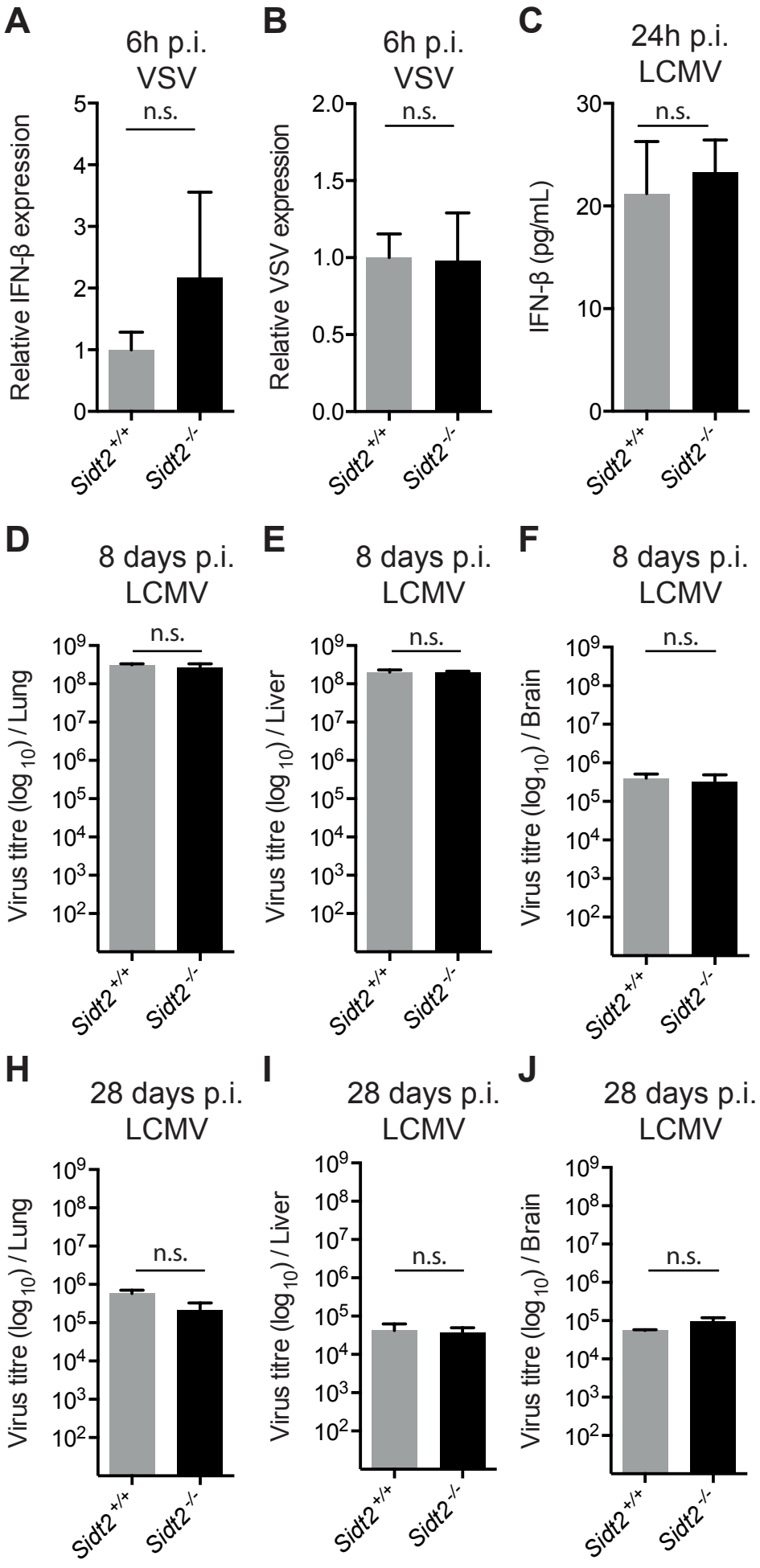
A
6h p.i.
VSV
n.s.
Relative IFN-β expression
Sidt2+/+
Sidt2-/-
B
6h p.i.
VSV
n.s.
Relative VSV expression
C
24h p.i.
LCMV
n.s.
IFN-β (pg/mL)
D
8 days p.i.
LCMV
n.s.
Virus titre (log10) / Lung
E
8 days p.i.
LCMV
n.s.
Virus titre (log10) / Liver
F
8 days p.i.
LCMV
n.s.
Virus titre (log10) / Brain
H
28 days p.i.
LCMV
n.s.
Virus titre (log10) / Lung
I
28 days p.i.
LCMV
n.s.
Virus titre (log10) / Liver
J
28 days p.i.
LCMV
n.s.
Virus titre (log10) / Brain

Figure S4 – Loss of SIDT2 does not impair innate immunity to VSV and LCMV.
(Related to Figure 2 and 3)

Sidt2$^{+/+}$ and *Sidt2*$^{-/-}$ mice (n=7-9) were infected with VSV via footpad injection, and **(A)** *Ifnβ* and **(B)** VSV mRNA within the draining popliteal lymph node were measured at 6 h p.i. by qRT-PCR and expressed relative to *Gapdh*. **(C)** *Sidt2*$^{+/+}$ and *Sidt2*$^{-/-}$ mice (n=5-7) were infected with LCMV (intravenous) and serum IFN-ß measured by ELISA at 24h p.i. **(D-F)** Viral titres in lung, liver and brain of mice 8 days **(D-F)** and 28 days **(H-J)** p.i. were measured via viral plaque assay. Data are plotted as mean ± SEM. n.s. = not significant. Serum IFN-ß was undetectable in uninfected mice.

Figure S5

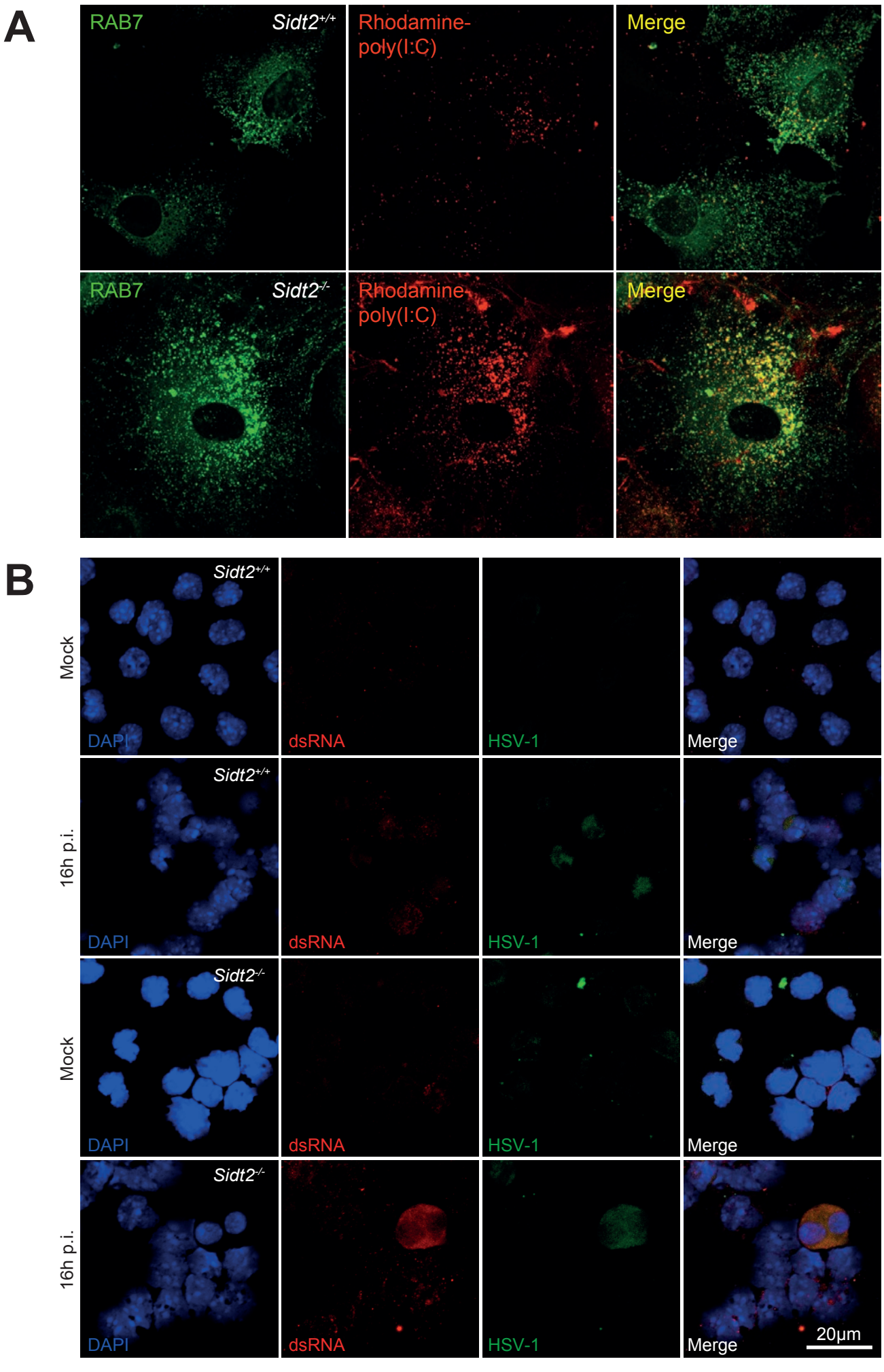
A
RAB7
Sidt2+/+
Rhodamine-poly(I:C)
Merge
RAB7
Sidt2-/-
Rhodamine-poly(I:C)
Merge
B
Mock
16h p.i.
Mock
16h p.i.
Sidt2+/+
Sidt2-/-
DAPI
dsRNA
HSV-1
Merge
20μm

Figure S5 – Loss of SIDT2 leads to accumulation of dsRNA.
(Related to Figures 4)
(A) MEFs from *Sidt2*$^{+/+}$ and *Sidt2*$^{-/-}$ mice stably were treated with poly(I:C)-rhodamine for 60 min, stained with an anti-Rab7 antibody (green), and analysed via confocal microscopy. Data are representative of 3 independent experiments. **(B)** Cells were retrieved via peritoneal lavage from *Sidt2*$^{+/+}$ and *Sidt2*$^{-/-}$ mice (n=3) infected with 1x10^{7} PFU HSV-1-GFP at 16 h p.i., stained with J2 dsRNA and DAPI antibody. Representative confocal images show localisation of HSV-1 dsRNA (red) in infected and uninfected cells.

Figure S6

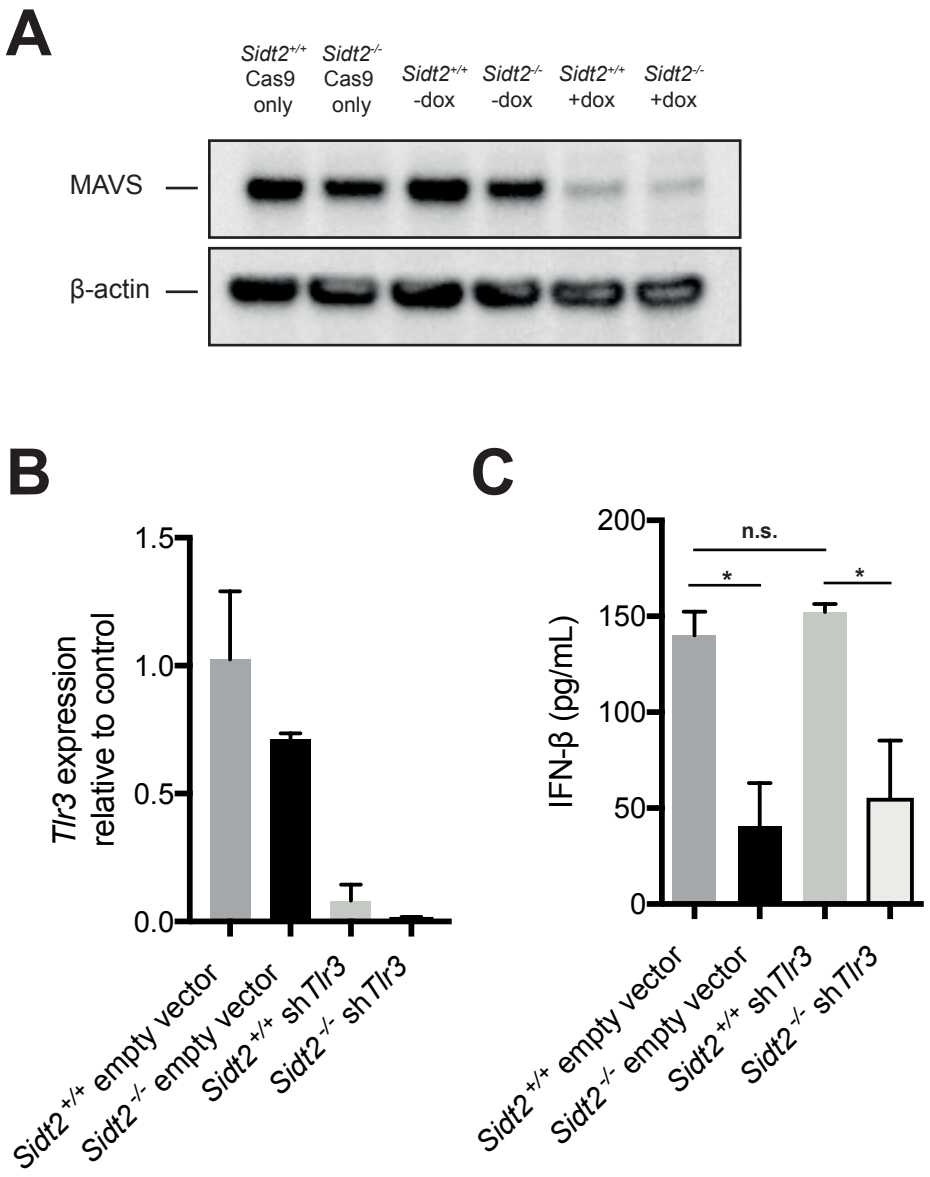
A
Sidt2+/+ Cas9 only
Sidt2-/- Cas9 only
Sidt2+/+ -dox
Sidt2-/- -dox
Sidt2+/+ +dox
Sidt2-/- +dox
MAVS
β-actin
B
Tlr3 expression relative to control
1.5
1.0
0.5
0.0
Sidt2+/+ empty vector
Sidt2-/- empty vector
Sidt2+/+ shTlr3
Sidt2-/- shTlr3
C
IFN-β (pg/mL)
200
150
100
50
0
n.s.
*
*
Sidt2+/+ empty vector
Sidt2-/- empty vector
Sidt2+/+ shTlr3
Sidt2-/- shTlr3

Figure S6 – Generation and assessment of of of *Sidt2*$^{-/-}$ *Mavs*$^{-/-}$ and *Sidt2*$^{-/-}$ sh*Tlr3* MEFs following HSV-1 infection.
(Related to Figure 7)
(A) Protein lysates from *Sidt2*$^{+/+}$ and *Sidt2*$^{-/-}$ MEFs that had been targeted by CRISPR (doxycycline-inducible) for Mavs were immunoblotted with MAVS antibody and protein loading was confirmed by blotting for β-actin**. (B)** RNA was prepared from *Sidt2*$^{+/+}$ and *Sidt2*$^{-/-}$ MEFs transduced with sh*Tlr3* or empty vector control and *Tlr3* expression normalised to expression *Gapdh* was measured by qRT-PCR and expressed relative to empty vector control. Data is plotted as ± SD. **(C)** sh*TLR3* and *Sidt2*$^{-/-}$ sh*TLR3* MEFs were infected with 1 MOI mCherry-tagged HSV-1 and IFN-β was measured in cell culture supernatant at 96 h p.i. via ELISA. *Sidt2*$^{+/+}$ and *Sidt2*$^{-/-}$ MEFs transduced with retroviral vector lacking shRNA (empty vector) were used as controls.

Figure S7

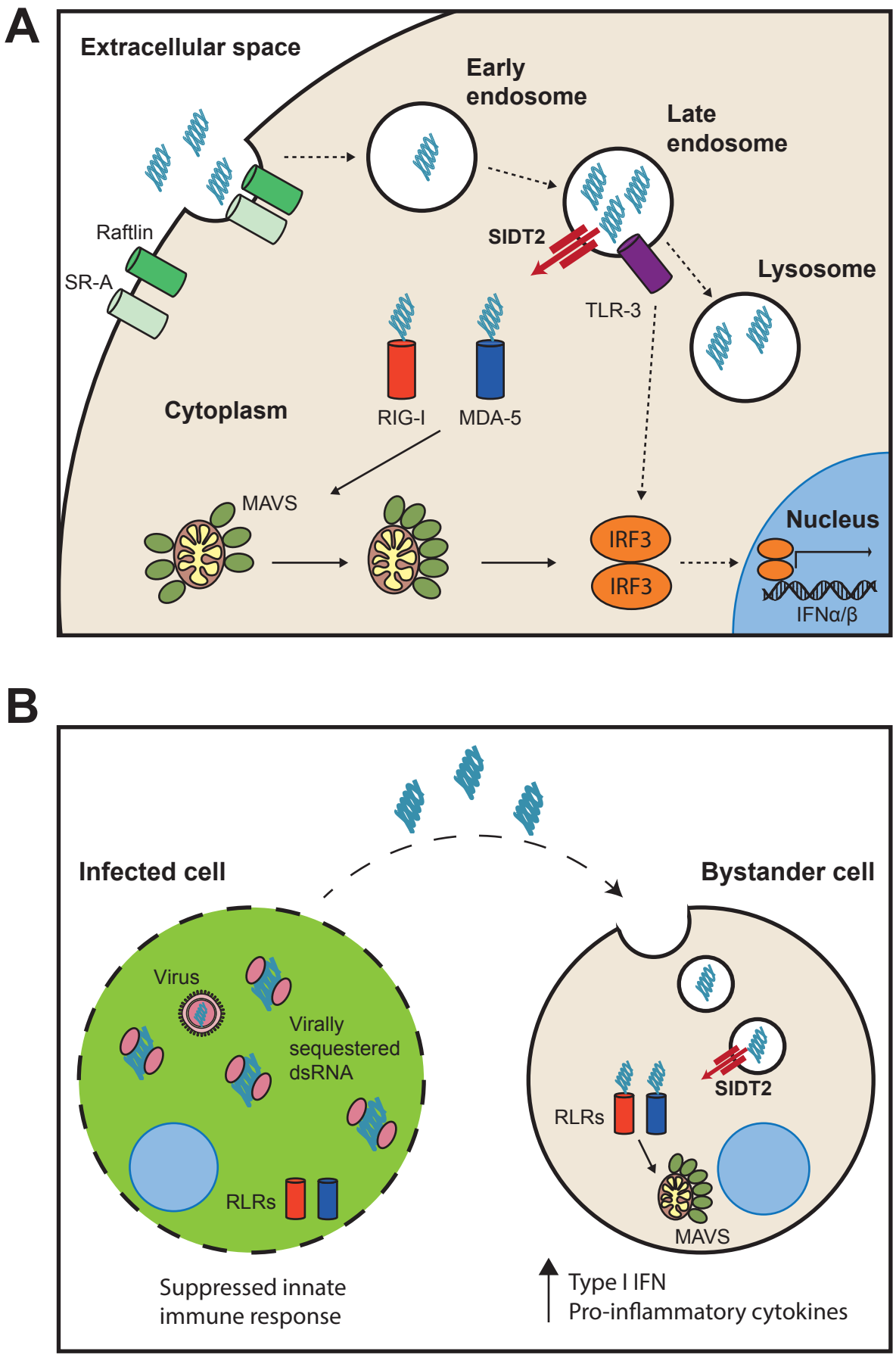
A
Extracellular space
Early endosome
Late endosome
Raftlin
SR-A
SIDT2
Lysosome
TLR-3
Cytoplasm
RIG-I
MDA-5
MAVS
IRF3
IRF3
Nucleus
IFNα/β
B
Infected cell
Bystander cell
Virus
Virally sequestered dsRNA
RLRs
SIDT2
RLRs
MAVS
Suppressed innate immune response
Type I IFN
Pro-inflammatory cytokines

Figure S7 – SIDT2 **facilitates the endosomal escape of internalised dsRNA for cytosolic sensing by the RLRs and bystander activation of innate immunity.**
(A) Upon internalisation via receptor-mediated endocytosis, extracellular dsRNA enters the endocytic pathway. SIDT2 transports this internalised dsRNA across the endosomal membrane into the cytoplasm, where it can be detected by RIG-I and MDA-5 leading to activation of MAVS and type I IFN production. Although endosomal dsRNA can also be sensed by TLR3, the contribution of this signalling pathway to type I IFN production following extracellular dsRNA exposure *in vivo* (e.g. poly(I:C)) is minor (Gitlin et al., 2006). **(B)** Viruses rely on multiple strategies to inhibit the innate immune response in infected cells leading to immune suppression in these cells. The transfer of dsRNA from infected cells to uninfected cells leads to SIDT2-dependent bystander activation of innate immunity via MAVS. The mechanisms by which dsRNA is transferred extracellularly remain to be determined, but might include cell lysis (e.g. due to the virus itself or immune destruction) and/or active release (e.g. via extracellular vesicles).

Table S1

Accession	Description
NP_001035545.1	SIDT2 [Homo sapiens] human
NP_060169.2	SIDT1 [Homo sapiens] human
NP_758461.1	SIDT2 [Mus musculus] mouse
EDK98036.1	SIDT1 [Mus musculus] mouse
*	SIDT2 [Xenopus tropicalis] frog
*	SIDT1 [Xenopus tropicalis] frog
XP_001233566.1	SIDT2 [Gallus gallus] bird
XP_416544.2	SIDT1 [Gallus gallus] bird
AAI55670.1	SIDT2 [Danio rerio] fish
XP_001520303.1	SIDT1 [Ornithorhynchus anatinus] platypus
XP_001502624.1	SIDT2 [Equus cabballus] horse
ACH970561.1	SID2 [Otolemur garnetti] bush baby
XP_002597180.1	SIDT-1/2 [Branchiostoma floridae] lancelet
NP_504372.2	SID-1 [Caenorhabditis elegans] nematode
XP_002636380.1	SID-1 [Caenorhabditis briggsae] nematode
XP_002645379.1	TAG-130 [Caenorhabditis briggsae] nematode
NP_509489.1	TAG-130 [Caenorhabditis elegans] nematode
XP_001605484.1	SID-1 [Natsonia vitripennis] wasp
NP_001099012.1	SID-1-related A [Tribolium castaneum] beetle
BAF95807.1	SID-1-like protein2 [Bombyx mori] moth
NP_001106736.1	SID-1 related gene3 [Bombyx mori] moth
XP_001951907.1	SID-1 [Acyrthosiphon pisum] aphid
ABP98803.1	SID-1 [Aphis gossypii] aphid
XP_002576874.1	SID-1 [Schistosoma mansoni] flatworm
XP_002114117.1	SID-1 [Trichoplax adhaerens] Placozoa
XP_002168603.1	SID-1 [Hydra magnipapillata] Cnidaria
XP_001742158.1	SID-1 [Monosiga brevicollis] Choanoflagelate
XP_001733041.1	SID-1 [Dictyostelium discoideum AX4] slime mold

SUPPLEMENTAL TABLES

Supplemental Table 1. Accession number and description of proteins used in Supplemental Figure 1.
** Xenopus tropicalis SidT1* and *SidT2* cDNA clones (IMAGE ID 7655239 and Sanger EST Clone ID TGas116o12) were obtained from Geneservice (www.geneservice.co.uk), and confirmed as full-length cDNAs by sequencing and comparison to EST clusters assembled in the Gordon Institute Full-Length database (Gilchrist et al., 2004). The corresponding protein sequences are listed below:

X. tropicalis SIDT1
MMAGMRPIWG NWILIFWLGT CAEALTRATG SKPAEFGKRY TGFVDKNTEE LYSFSYTSKN
DTVDALRVFV SSNSINLEFP VLFVVRQQKA ILSWQVPMVF RGNFPRTYTY QDVSRTLCPT
EPEEGTGSQE QFIYIDIASM SPSIVQYELM VTRLLSFQLK TSVPFNFSAS PSQPQYFLYT
FPEGVDSVII KVKSPENYPC SVVSVQDISC PVYDLDYNVE FNGVYQTMTK QAAITVQRKE
YPGGKFYVVF VIKPEDYTCG GTVPQSTQGS GNHTWNLKRV KHMEVTVSPS VKDSVYVQAT
LLCLLYFLIF YVGSLLVAFV HYVSIHRKER NLKGSPDEGE GTVAASHPIT TSTPDGSSYG
AIDESSPGAR KMTPPPIPRP RVYSDSSADE ESDFDAIPEM ETDKNVIRAK TFLYVSDLAV
KDRRVVSKKY RIYFWNIITI AVFYALPVVQ LVITYQTVLN VTGNQDICYY NFLCAHPLGV
LSAFNNVMSN MGHVLLGFLF LLIVLRRDLL HRHLLEVNDT YAKDYGIPKH FGLFYTMGVA
LIMEGVLSAC YHVCPNYSNF QFDTSFMYMI AGLCMLKLYQ TRHPDINASA YAAYASFALV
IFLAVMGVIF GKDNIWFWVI FSIVHVVGSL ALSTHIYYMG RFRIDVSNAD FGIFKRIAQV
LYTDCMQQCS RPMYMDRMIL LIVGNIVNWL FAIFGLVFRP RDFPSYLLGI FICNLLLYLA
FYIIMKLRSS ERIQTLPLFC IIATAVVWAA ALYFFFQTLS SWEQTPAESR EKNRSCIILH
FFDDHDIWHF LSATAMFFSF LVLLTLDDDL DVVRRDKIPV F

X. tropicalis SIDT2
MPVFGVLLLI WHIGLSLGGN TYFQDKVIVQ KNAEFNKEYN DSVNAEQQNI YAFNHTMLRN
KTDGVRVSVN VLSDQKATPL LFVVRQKEAV VSFQVPLALR GQYQRNYLYQ DVGRTLCQPP
TRAEAETESF YVDVSTLAEK NTTYRLRVTH VENFVLQTNG PFNFNATPAQ PQYFKYLFPE
GVESVIVKVS SSSVFPCSVI SVQDIQCPVY DLDNNVAFIG MYQTMTKKAA ITVQRKDFSS
GGFYVVVVVK TEDEACGGAL PLFPLHQDIP VDHLSRQKNL EVLVSPAINR NVYVAGMLFC
LGVFLSFYLV ALLISCWEQY RKKNKSEDPF LNSASSLNDE TASLLGKPPM CPKYDACGYG
SIAAQHSSSV PSPEDCTDSL VSSGEATYSY TDRSLENLVS RNRLESLSSV EEDDYDTLTD
IESDKNVIRT KKFLCVSDLA RKDKRVMRKK YQIYFWNIST IAVFYALPVI QLVITYQTVV
NVTGNQDICY YNFLCAHPLG SLSAFNNILS NLGYVMLGLL FLVIVLQREL SHNHNRMNIR
GQLQECGIPK HFGLFYAMGT ALMMEGLLSA CYHVCPNYTN FQFDTSFMYM IAGLCMLKLY
QKRHPDINAS AYSAYACLAI VIFFSVVGVV FGNGNTIFWV VFSVIHILFT LLLSTQLYYM
GRWRLDSAIL RRIFHVLYTD CVRQCSPPMY VDRMVLLVMG NIVNWSLAAY GLIVRPKDFA
SYLLAIGICN LLLYFAFYII MKLRSGERIL PIPLLCITCT SVVWGFALFF FFQGLSTWQK
TPAESREHNR NCILLGFFDD HDIWHFLSSI AMFGSFLVLL FLDDDLDSVQ RDKIFVF

GVESVIVKVS SSSVFPCSVI SVQDIQCPVY DLDNNVAFIG MYQTMTKKAA ITVQRKDFSS
GGFYVVVVVK TEDEACGGAL PLFPLHQDIP VDHLSRQKNL EVLVSPAINR NVYVAGMLFC
LGVFLSFYLV ALLISCWEQY RKKNKSEDPF LNSASSLNDE TASLLGKPPM CPKYDACGYG
SIAAQHSSSV PSPEDCTDSL VSSGEATYSY TDRSLENLVS RNRLESLSSV EEDDYDTLTD
IESDKNVIRT KKFLCVSDLA RKDKRVMRKK YQIYFWNIST IAVFYALPVI QLVITYQTVV
NVTGNQDICY YNFLCAHPLG SLSAFNNILS NLGYVMLGLL FLVIVLQREL SHNHNRMNIR
GQLQECGIPK HFGLFYAMGT ALMMEGLLSA CYHVCPNYTN FQFDTSFMYM IAGLCMLKLY
QKRHPDINAS AYSAYACLAI VIFFSVVGVV FGNGNTIFWV VFSVIHILFT LLLSTQLYYM
GRWRLDSAIL RRIFHVLYTD CVRQCSPPMY VDRMVLLVMG NIVNWSLAAY GLIVRPKDFA
SYLLAIGICN LLLYFAFYII MKLRSGERIL PIPLLCITCT SVVWGFALFF FFQGLSTWQK
TPAESREHNR NCILLGFFDD HDIWHFLSSI AMFGSFLVLL FLDDDLDSVQ RDKIFVF